

## Time-spatial variability observed in velocity of propagation of the internal bore in the Strait of Gibraltar

J. C. Sánchez Garrido,<sup>1,2</sup> J. García Lafuente,<sup>1</sup> F. Criado Aldeanueva,<sup>1</sup>  
A. Baquerizo,<sup>2</sup> and G. Sannino<sup>3</sup>

Received 6 November 2007; revised 31 January 2008; accepted 27 February 2008; published 24 July 2008.

[1] Some aspects of the time-spatial variability of the phase speed of the internal bore generated almost every tidal cycle in Camarinal Sill, are revised using a set of high resolution experimental data collected in two different positions of the Strait during May 2003. This variability is mainly driven by the intense tidal currents, comparable with the intrinsic propagation velocity of the first mode baroclinic bore. It is shown that the importance of the diurnal tide in the Strait of Gibraltar induces a considerable diurnal inequality on the bore velocity, with an observed maximum difference of  $0.7 \text{ ms}^{-1}$  between the speed of two consecutive bores propagating along the eastern part of the Strait. A regularly spatial pattern has been also found: the internal bore reaches its maximum velocity in Tarifa Narrows. A theoretical estimation predicts an extreme phase speed of  $2.6 \text{ ms}^{-1}$  during our period of study.

**Citation:** Sánchez Garrido, J. C., J. García Lafuente, F. Criado Aldeanueva, A. Baquerizo, and G. Sannino (2008), Time-spatial variability observed in velocity of propagation of the internal bore in the Strait of Gibraltar, *J. Geophys. Res.*, *113*, C07034, doi:10.1029/2007JC004624.

### 1. Introduction

[2] The Strait of Gibraltar, the only connection between the Atlantic Ocean and the Mediterranean Sea, is a well known scenario of inverse estuarine circulation, with an undercurrent of colder and saltier Mediterranean water (MW) flowing at depth toward the Atlantic and a surface current of warmer and fresher Atlantic water (AW) moving opposite exceeding slightly the deep flow to compensate the net evaporative loses in the Mediterranean reservoir [Lacombe and Richez, 1982; Bryden and Kinder, 1991; García Lafuente *et al.*, 2002]. Although the main focus of study has been the long-term exchange due to the role the MW could play in the global circulation and to follow the climate variability in the Mediterranean Sea area [Candela, 2001; García Lafuente *et al.*, 2007], the internal tide and associated mixing in the Strait has also been a widely revised topic [Ziegenbein, 1969, 1970; La Violette and Arnone, 1988; Farmer and Armi, 1988; Richez, 1994; Bruno *et al.*, 2002; Morozov *et al.*, 2002; Vázquez *et al.*, 2006]. The stratification originated by the salinity contrast between AW and MW, the intense tidal currents and the abrupt topography of the Strait of Gibraltar (see Figure 1) convert this place in a very favorable environment for the generation of large amplitude internal tides and tidally related internal perturbations, among which the internal hydraulic jump formed at the lee side of Camarinal sill

(Figure 1) during the flood tide (tidal currents toward the Atlantic) is the most outstanding one [Farmer and Armi, 1988]. The jump remains trapped by the flow, extracting energy from the background current, until the tidal current weakens and the flow becomes subcritical over the sill, which happens shortly before high water (HW). In addition to tidal forcing, the time of the bore release is also influenced by other factors, mainly the subinertial meteorological forcing, as showed by Pistek and La Violette [1999]. After its release, the internal jump propagates as an internal bore toward the Mediterranean Sea and starts disintegrating into a packet of solitary internal waves (SIWs).

[3] During its progression toward the Mediterranean Sea, the packet of SIWs undergoes different conditions of stratification, variable tidal currents and mean flow that determine the time-space variability of the internal bore velocity. Tidal influence on the variability was found by Watson and Robinson [1990], who observed a remarkable diurnal inequality in the time arrival of internal waves to Gibraltar due to the relative intense diurnal tidal currents [García Lafuente *et al.*, 2000]. Recent numerical studies have also shown the existence of a location between Tarifa and Punta Cires (Figure 1) where the propagation speed of the bore reaches a maximum [Brandt *et al.*, 1996; Izquierdo *et al.*, 2001; Sannino *et al.*, 2004]. The analysis of the time-space variability of the internal bore velocity using observations of temperature and flow velocity in two locations of the Strait of Gibraltar is the scope of this paper.

### 2. Data Set

[4] During May 2003, two mooring lines were deployed in two strategic positions of the Strait of Gibraltar, one in

<sup>1</sup>Grupo de Oceanografía Física, University of Málaga, Málaga, Spain.

<sup>2</sup>Grupo de Puertos y Costas, University of Granada, Granada, Spain.

<sup>3</sup>Climate Department, ENEA, C.R. Casaccia, Rome, Italy.

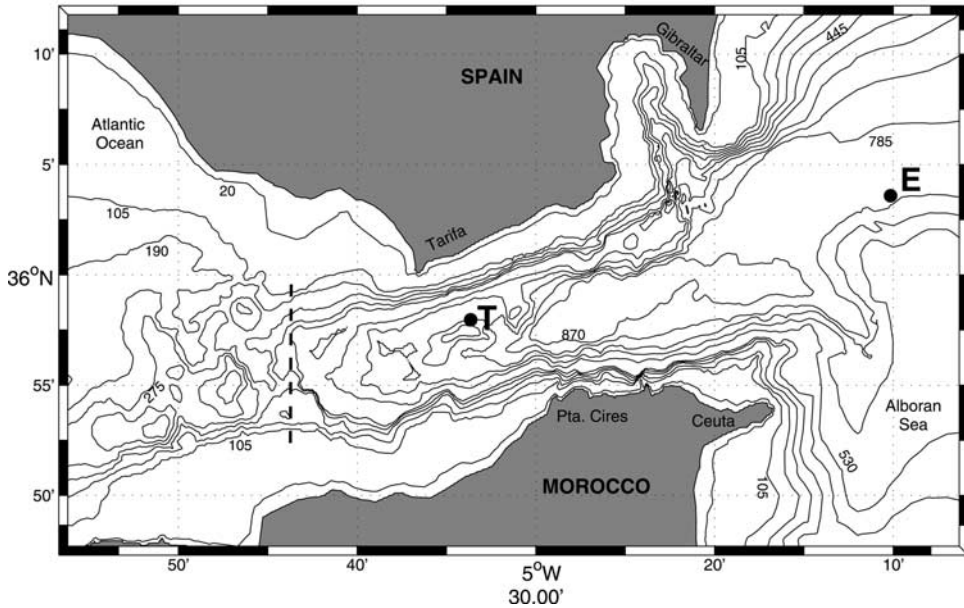


**Figure 1.** Bottom topography of the Strait of Gibraltar. Location of stations are indicated with letters T and E. Dashed line indicates the section of Camarinal Sill.

Tarifa narrows, the section of minimum width of the Strait, at  $35^{\circ}57.58'N$ ,  $5^{\circ}32.99'W$  (T in Figure 1) and the other in the entrance of the Alboran Sea at  $36^{\circ}3.35'N$ ,  $5^{\circ}10.09'W$  (E in Figure 1). The mooring array consisted of several currentmeters at different depths that measured velocity and temperature every 2 or 5 min (see Table 1 for details). For unknown reasons, the mooring line in point T broke beneath the second uppermost instrument 22 d after deployment and the remaining instruments of the line fell down to the seafloor doing senseless observations. The two shallowest currentmeters were lost. Conductivity-Temperature-Depth profiles in the Strait were retrieved from MEDATLAS database [MEDAR Group, 2002] for May months in order to obtain a monthly climatology of the area. The numerical model described by Sannino et al. [2004] was run using improved bathymetry and different initial and tidal forcing. The main diurnal ( $O_1$ ,  $K_1$ ) and semidiurnal ( $M_2$ ,  $S_2$ ) tidal constituents have been computed via OTIS package [Egbert and Erofeeva, 2002] while initial conditions, in terms of salinity and temperature, have been also taken from MEDATLAS database. The model provided continuous vertical profiles of the background flow at specific places that have been used subsequently to analyze the observations.

### 3. Identification of SIWs

[5] Internal waves at station E are clearly depicted by the temperature series collected by RCM E2 at 85 m depth (Figure 2a). Throughout the time series, peaks with semi-diurnal periodicity are observed except around days 130 and 145 that correspond to neap tides. The zoom of the series showed in Figure 2b reveals the short period oscillations associated with SIW packets. Internal waves are less sharply detected in the temperature series at site T. The reason is that the recovered instruments were well below the thermocline (located at 80 m depth according to CTD data) in depths where the vertical gradient of temperature is small.

The equation of conservation of thermal energy, neglecting thermal diffusion and horizontal gradients of temperature,

$$\frac{\partial T}{\partial t} = -w \frac{\partial T}{\partial z} \quad (1)$$

indicates that temporal variations of temperature are imperceptible in homogeneous regions. However, high frequency motions are recognizable in velocity time series at T. Figure 2c shows the horizontal velocity collected at T4, which follows the ebb and flood cycles quite regularly. The enlargement showed in Figure 2d reveals disturbances linked to the internal bore and SIWs packets about 6 h before they pass through position E.

### 4. Influence of the Diurnal Inequality

[6] Watson and Robinson [1990] monitored the arrival of SIW to Gibraltar by means of shore based marine radar during 3 months. They noted a remarkable difference

**Table 1.** Arrangement of the Mooring Lines Used in the Study

Currentmeter	Depth, m	Sampling Interval, min
T1	156	2
T2	204	2
T3	250	5
T4	341	5
Station E (01 May 2003 to 3 Jun 2003; $36^{\circ}3.35'N$ , $5^{\circ}10.09'W$ )		
E1	52	2
E2	85	2
E3	116	2
E4	166	2
E5	231	5
E6	348	5

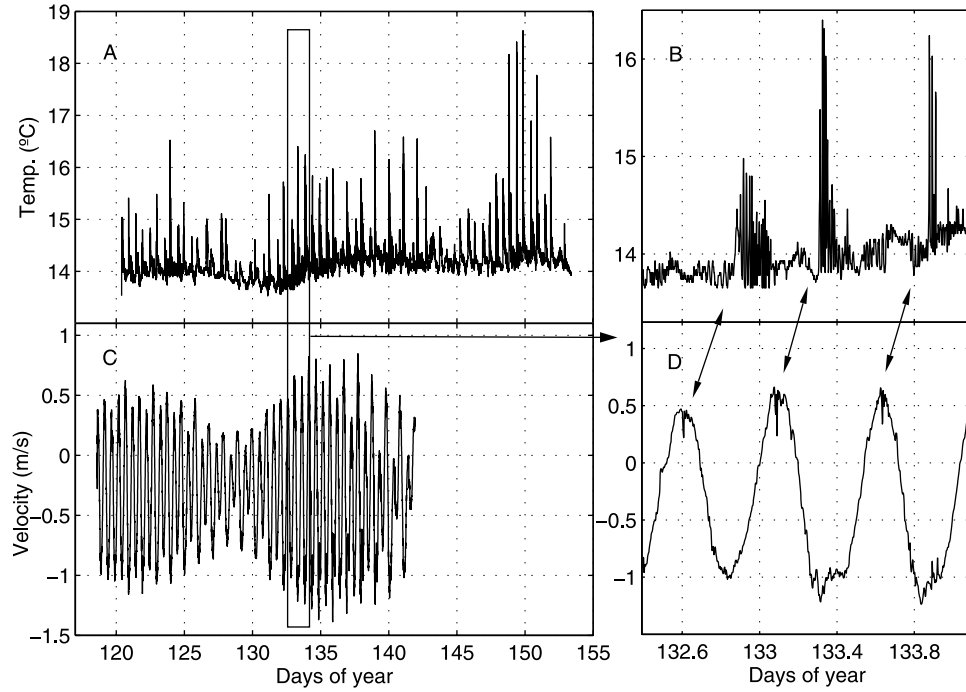


**Figure 2.** (a) Temperature recorded at 85 m depth in site E (RCM E2). (b) Enlargement of the section selected in Figure 2a. (c) Along-strait component of the velocity recorded at 341 m depth in site T (RCM T4). (d) Enlargement of the section selected in Figure 2c. Double arrows in Figures 2b–2d point at the signatures left by the same internal wave packets in both stations.

between the arrival time of two consecutive SIWs packets after high water. The difference was maximum (about 8 h) during periods of diurnal spring tides, and null during periods of diurnal neap tides. It was then suggested that the horizontal advection by diurnal tidal currents exerts an important influence on the propagation velocity of the internal bore. In the Strait of Gibraltar, the main diurnal tidal constituents  $K_1$  and  $O_1$  account for an important part of the total barotropic tidal energy [García Lafuente et al., 2000; Sánchez Román et al., 2008].

[7] This result is strongly supported by our observations. Figures 3a and 3b show the time arrival of SIWs, measured from the immediately previous HW (Ceuta is the reference harbor for HW throughout this paper), to stations E and T respectively. They arrive to position E between 5–12 h after HW, whereas they get position T 0.5–4.5 h after HW. Events of SIWs corresponding to odd and even semidiurnal cycles have been joined together with different line style to highlight the diurnal inequality. The diurnal age, the lag between the extreme moon declination and its maximum effect on the tidal range, is determined by the phase difference of  $K_1$  and  $O_1$  constituents. In the eastern half of the Strait the difference is around  $50^\circ$  [García Lafuente et al., 1990] and the diurnal age is around 2 d. The diurnal inequality reaches its maximum 2 d after the extreme values of the declination of the moon, which happened in 6 May (maximum declination) and 19 May (minimum), or Julian days 127 and 140 respectively. Minimum delay after HW is then expected to occur in one of the two semidiurnal cycles (and maximum delay in the other one) near Julian days 129 and 142 and, in fact, Figure 3a shows this minimum (maximum) in odd (even) cycles around day 128 and in

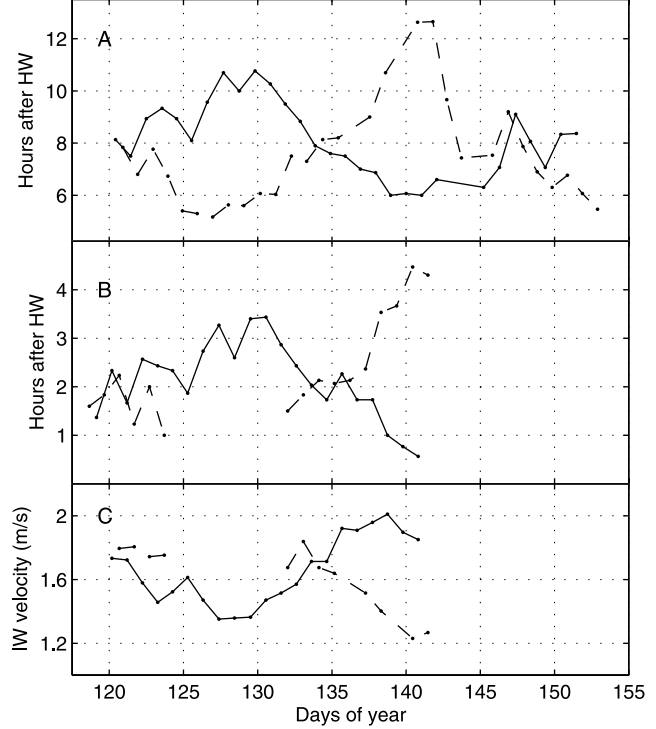


**Figure 3.** Arrival of the internal bore, referred to the previous high water, at station E (a) and T (b). (c) mean propagation speed of the internal bore between stations T and E. Events corresponding to even and odd semidiurnal cycles have been joined together using dotted and solid lines respectively to highlight the evolution of the diurnal inequality (see text for details).

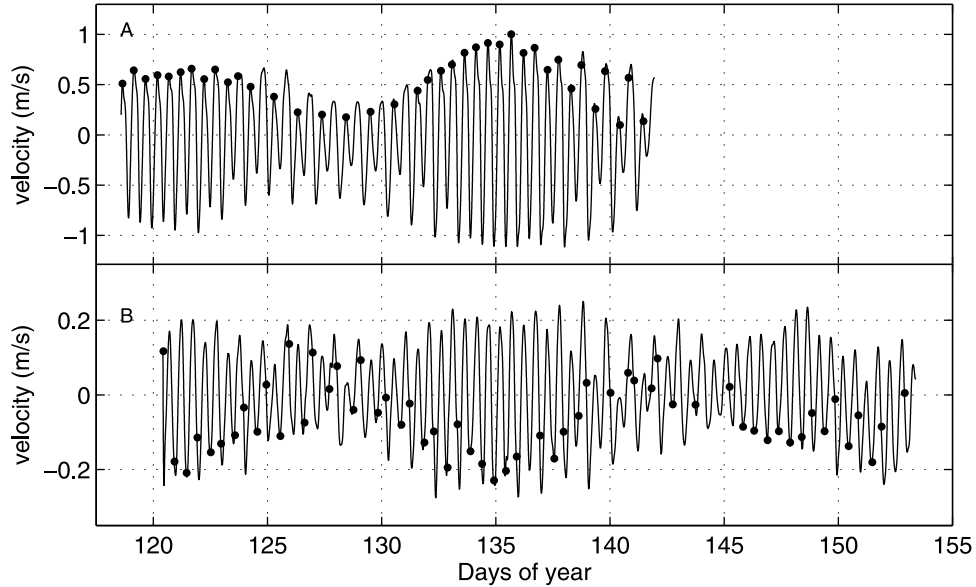


**Figure 4.** Barotropic contribution of the along-strait component of the tidal currents at stations T (a) and E (b) deduced from EOF analysis. Dots indicate the time when SIWs are identified in either station. In station T, SIWs find the most favorable current conditions with regularity.

even (odd) cycles near day 141 (notice that diurnal inequality changes from odd to even cycles when the moon passes over the Equator, which happens around day 134). Figure 3b does not illustrate this behavior as nicely as Figure 3a since velocity is less sharp indicator of SIWs pass. The mean propagation speed of the internal bore between T and E (separated 36 km) has also been straightforward calculated in those tidal cycles when internal waves were tracked in both stations. Speed ranges from  $1.2$  to  $2\text{ ms}^{-1}$  mainly due to the diurnal inequality (Figure 3c).

## 5. Local Maximum Speed in Site T

[8] The result produced by numerical experiments that the internal bore propagates faster in the surrounding of station T due to the influence of tidal currents [Brandt *et al.*, 1996; Izquierdo *et al.*, 2001; Sannino *et al.*, 2004] is investigated next from our data set.

[9] One commonly used statistical procedure to extract the barotropic contribution from time series of velocity is the Empirical Orthogonal Functions (EOF) analysis, which decomposes the signals into empirical orthogonal modes. The analysis has been carried out to the along-strait component of the velocity in both stations after removing noise and high frequencies oscillations not directly linked with tides (by means of a butterworth filter with cut off period 3 h). At T, the first empirical mode does not reveal any remarkable spatial structure, that is, it is nearly z-independent with no zero-crossing, which can therefore be identified with the barotropic mode. It explains 85% of the variance, and its temporal coefficients are plotted in Figure 4a. As far as the spatial coefficients have been normalized, the physical units are included in the time coefficients of Figure 4a, which therefore represents the amplitudes of the barotropic mode. It reaches values as high as  $1\text{ ms}^{-1}$ . Dots in the figure indicate

the arrival of wave packets at station T and confirms that, indeed, the SIWs meet the most favorable tidal conditions ( $0.14 \pm 0.84\text{ h}$  before the maximum inflow) to progress faster toward the Mediterranean in this site, in agreement with the aforementioned numerical references. Figure 4b shows the barotropic mode in station E and the arrival of SIWs at this site. The maximum tidal amplitude is less than  $0.25\text{ ms}^{-1}$  and the location of the dots throughout the curve indicates that on average SIWs face unfavorable tidal currents to progress eastward, which diminishes its propagation speed.

## 6. Propagation Speed From Analytical Models

[10] Due to the relatively intense currents associated with the mean exchange in the Strait of Gibraltar a first estimate of the speed of the internal bore could be computed from the Taylor Goldstein equation, which provides the modal structure of a linear perturbation in a stable shear flow. Under the Boussinesq approximation, it reads:

$$\frac{d}{dz} \left[ (U - c_j)^2 \frac{dW_j}{dz} \right] + \left[ N^2 - k^2(U - c_j)^2 \right] \cdot W_j = 0, \quad (2)$$

where  $N(z)$  is the buoyancy frequency,  $U(z)$  the long-term mean of the along-strait velocity profile,  $W_j(z)$  the  $j$ -th vertical mode,  $k$  the wave number, and  $c_j$  the linear phase speed. Figures 5a–5b show averaged  $N$  profiles for stations T and E obtained from MEDATLAS database. The long-term  $U(z)$  velocity in equation (2) could be somewhat approximated from the time averaged values of the registered data by interpolation/extrapolation (see Figure 5). On the other hand, the vertical profile of horizontal velocity achieved by averaging the model output during 1 month, matches closely the observations at the different depths (see solid line in Figure 5). For this reason, the  $U(z)$  averaged profile of the

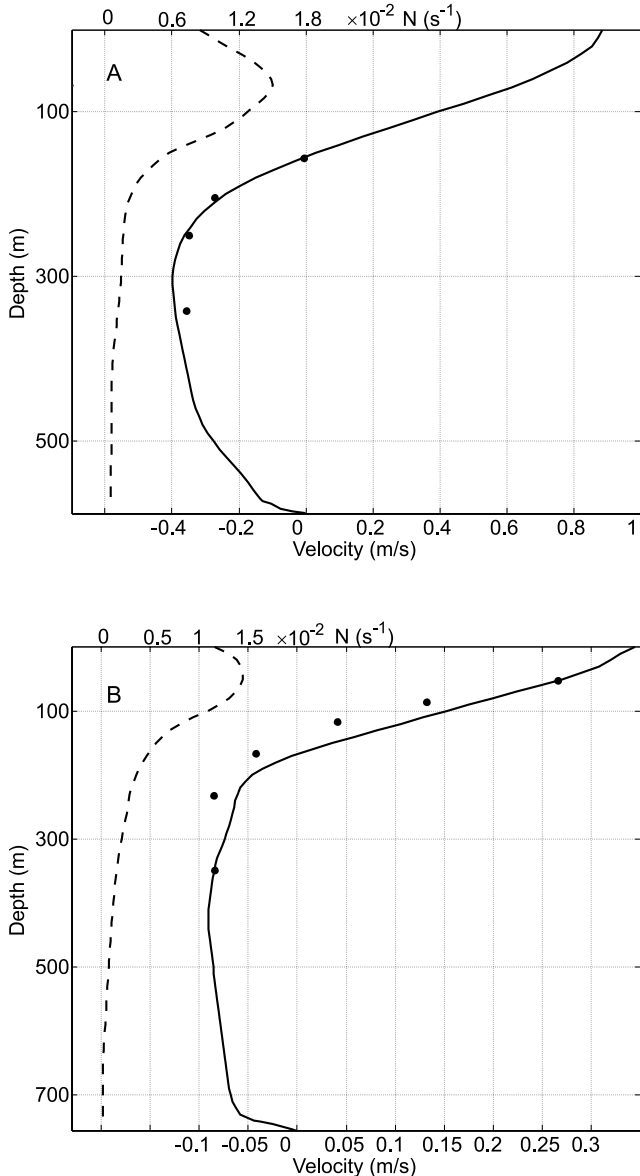


**Figure 5.** (a) Buoyancy frequency from MEDATLAS database (dashed line, top scale) and vertical profile of the long-term along-strait velocity from the numerical model (solid line, bottom scale) in station T. Dots indicate the mean velocity recorded by the instruments. (b) Same as Figure 5a for station E.

model, which has much better spatial resolution, has been used instead.

[11] The equation has been solved for long-wave approximation ( $k \sim 0$ ) imposing rigid lid boundary conditions ( $W_j(-H) = W_j(0) = 0$ ;  $H$  being the water depth) since we are only interested in baroclinic modes. The propagation speed of the first mode in stations T and E are  $1.62$  and  $1.23 \text{ ms}^{-1}$ , respectively. Since stratification is similar in both locations, the difference must be ascribed to the higher upper layer velocity at station T (about  $0.8 \text{ ms}^{-1}$ , Figure 5a). If the influence of the barotropic tidal current derived in section 5 is taken into account and added to the previous calculations,

the propagation speeds would range between  $1.72$ – $2.62 \text{ ms}^{-1}$  at T and  $1.0$ – $1.37 \text{ ms}^{-1}$  at E. These values agree with the experimental observations (Figure 3c).

[12] The internal tide in the Strait of Gibraltar cannot be satisfactorily described by linear theory. In fact, the disintegration of the internal bore into SIWs packets is an unequivocal signature of nonlinear effects. A theoretical approximation often used to describe nonlinear internal waves is the weakly nonlinear dispersive Korteweg-de Vries (K-dV) theory. It holds provided that the so-called nonlinear,  $\varepsilon = a/H$ , and dispersive,  $\mu = (H/\lambda)^2$ , parameters ( $a$  the wave amplitude,  $\lambda$  the wavelength) are much less than one.

[13] The large amplitude internal waves reported in the Strait of Gibraltar [Ziegelnbein, 1969, 1970; Vázquez et al., 2006] fulfil only partially the conditions for the validity of this theory. However, Vlasenko et al. [2000] found that K-dV theory provides a satisfactory approximation to nonlinear speed of solitons whenever the vertical density gradient is relatively weak. The stratification showed in Figure 5a varies slowly within the first 200 m, with a maximum  $N_{\max} = 1.5 \cdot 10^{-2} \text{ s}^{-1}$ , which is similar to the stratification used by Vlasenko et al. [2000].

[14] Within the first order K-dV theory, the nonlinear phase velocity of a solitary wave  $c_{NL}$  is

$$c_{NL} = c_j + \frac{\alpha \cdot a}{3} \quad (3)$$

where  $\alpha$  is the coefficient of nonlinearity in the K-dV equation defined as

$$\alpha = \frac{3 \int_{-H}^0 (U - c_j)^2 \left( \frac{dW_j}{dz} \right)^3}{2 \int_{-H}^0 (U - c_j) \left( \frac{dW_j}{dz} \right)^2} \quad (4)$$

under the Boussinesq approximation [Grimshaw et al., 2002].

[15] For stations T and E,  $\alpha_T = 3.20 \cdot 10^{-3} \text{ m}^{-1}$  and  $\alpha_E = 1.02 \cdot 10^{-2} \text{ m}^{-1}$ , respectively. For extreme large solitary waves of 100 m amplitude, K-dV equation only predicts an increment of 7% of the linear phase velocity at station T and a higher increase of 27% at station E. In this last station, however, the wave radiation caused by the widening of the topography reduces the amplitude of the wave, thus balancing the increase introduced by parameter  $\alpha$ . Therefore in both cases nonlinear effects are not expected to substantially increase the linear phase speed.

## 7. Summary and Conclusions

[16] A high resolution experimental data of current velocity and temperature collected in the Strait of Gibraltar have been analyzed in order to study the time-space variability of the propagation speed of the tidally generated internal bore. Diurnal species induce an important diurnal inequality on the internal bore velocity associated with the declination of the moon, a result already mentioned by other authors [Watson and Robinson, 1990; Richez, 1994]. During

our experiment, phase speed of SIWs packets propagating along the eastern half of the Strait linked to two consecutive semidiurnal cycles can differ more than  $0.7 \text{ ms}^{-1}$ . It has been also shown that SIWs regularly reach maximum speed nearby Tarifa narrows because the wave packets are progressing through this area when the tidal current peaks toward the Mediterranean Sea. A theoretical approximation derived from linear theory along with tidal advection deduced from the analysis indicate that phase speed can exceed  $2.6 \text{ ms}^{-1}$  in this area during the period of study. Nonlinear theory has also been considered to compute the propagation speed more accurately but its contribution does not turn out to be very different from the prediction of linear theory.

[17] **Acknowledgments.** JCSG acknowledges a postgraduate fellowship from Consejería de Innovación Ciencia y Empresa, Junta de Andalucía, Spain. We acknowledge the project RNM 968 funded by this Consejería, and the projects REN03-01608/MAR, CTM2006-02326/MAR, funded by the Spanish Ministerio de Educación y Ciencia.

## References

- Brandt, P., W. Alpers, and J. O. Backhaus (1996), Study of the generation and propagation of internal waves in the Strait of Gibraltar using a numerical model and synthetic aperture radar images of the European ERS 1 satellite, *J. Geophys. Res.*, **101**, 14,237–14,252.
- Bruno, M., J. J. Alonso, A. Cázar, J. Vidal, A. Ruiz-Cañavate, F. Echevarría, and J. Ruiz (2002), The boiling-water phenomena at Camarinal sill, the Strait of Gibraltar, *Deep Sea Res., Part II*, **49**, 4097–4113.
- Bryden, H. L., and T. H. Kinder (1991), Steady two-layer exchange through the Strait of Gibraltar, *Deep Sea Res., Part I*, **38**, S1, S445–S463.
- Candela, J. (2001), Mediterranean water and global circulation, in *Ocean Circulation and Climate*, edited by G. Siedler, J. Church, and J. Gould, pp. 419–429, Elsevier, New York.
- Egbert, G., and L. Erofeeva (2002), Efficient inverse modeling of barotropic ocean tides, *J. Atmos. Oceanic Technol.*, **19**, 183–204.
- Farmer, D., and L. Armi (1988), The flow of Mediterranean water through the Strait of Gibraltar; the flow of Atlantic water through the Strait of Gibraltar, *Prog. Oceanogr.*, **21**, 1–106.
- García Lafuente, J., J. L. Almazán, F. Castillejo, A. Khribiche, and A. Hakimi (1990), Sea level in the Strait of Gibraltar: Tides, *Int. Hydrogr. Rev.*, **47**, 111–130.
- García Lafuente, J., J. M. Vargas, F. Plaza, T. Sarhan, J. Candela, and B. Baschek (2000), Tide at the eastern section of the Strait of Gibraltar, *J. Geophys. Res.*, **105**, 14,197–14,213.
- García Lafuente, J., E. Alvarez Fanjul, J. M. Vargas, and A. W. Ratsimandresy (2002), Subinertial variability in the flow through the Strait of Gibraltar, *J. Geophys. Res.*, **107**(C10), 3168, doi:10.1029/2001JC001104.
- García Lafuente, J., A. Sánchez Román, G. Díaz del Río, G. Sannino, and J. C. Sánchez Garrido (2007), Recent observations of seasonal variability of the Mediterranean outflow in the Strait of Gibraltar, *J. Geophys. Res.*, **112**, C10005, doi:10.1029/2006JC003992.
- Grimshaw, R., D. Pelinovsky, and O. Poloukhina (2002), Higher-order Korteweg-de Vries models for internal solitary waves in a stratified shear flow with a free surface, *Nonlinear Proc. Geophys.*, **9**, 221–325.
- Izquierdo, A., L. Tejedor, D. V. Sein, J. O. Backhaus, P. Brandt, A. Rubino, and B. A. Kagan (2001), Control variability and internal bore evolution in the Strait of Gibraltar: A 2-D two-layer model study, *Estuarine Coastal Shelf Sci.*, **53**, 637–651.
- Lacombe, H., and C. Richez (1982), The regime of the Strait of Gibraltar, in *Hydrodynamics of Semi-Enclosed Seas*, edited by J. C. J. Nihoul, pp. 13–74, Elsevier, Amsterdam.
- La Violette, P. E., and R. A. Arnone (1988), A tide-generated internal waveform in the western approaches to the Strait of Gibraltar, *J. Geophys. Res.*, **93C**, 15,653–15,667.
- MEDAR Group (2002), MEDATLAS/2002 database, Mediterranean and Black Sea database of temperature salinity and bio-chemical parameters, *Climatological Atlas*, IFREMER Edition.
- Morozov, E., K. Trulsen, M. Velarde, and V. Vlasenko (2002), Internal tides in the Strait of Gibraltar, *J. Phys. Oceanogr.*, **32**, 3193–3206.
- Pistek, P., and P. La Viollete (1999), Observations of the suppression of tide-generated nonlinear internal wave packets in the Strait of Gibraltar, *J. Mar. Syst.*, **20**, 113–128.
- Richez, C. (1994), Airbone synthetic aperture radar tracking of internal waves in the Strait of Gibraltar, *Prog. Oceanogr.*, **33**, 93–159.
- Sánchez Román, A., F. Criado Aldeanueva, J. García Lafuente, and J. C. Sánchez Garrido (2008), Vertical structure of tidal currents over Espartel and Camarinal Sill, Strait of Gibraltar, *J. Marine. Syst.*, doi:10.1016/j.jmarsys.2007.11.007, in press.
- Sannino, G., A. Bargagli, and V. Artale (2004), Numerical modelling of the semidiurnal tidal exchange through the Strait of Gibraltar, *J. Geophys. Res.*, **109**, C05011, doi:10.1029/2003JC002057.
- Vázquez, A., N. Stashchuk, V. Vlasenko, M. Bruno, A. Izquierdo, and P. C. Gallacher (2006), Evidence of multimodal structure of the baroclinic tide in the Strait of Gibraltar, *Geophys. Res. Lett.*, **33**, L17605, doi:10.1029/2006GL026806.
- Vlasenko, V. I., P. Brandt, and A. Rubino (2000), On the structure of large-amplitude internal solitary waves, *J. Phys. Oceanogr.*, **30**, 2172–2185.
- Watson, G., and I. S. Robinson (1990), A study of internal waves propagation in the Strait of Gibraltar using shore-based radar images, *J. Phys. Oceanogr.*, **20**, 374–395.
- Ziegenein, J. (1969), Short internal waves in the Strait of Gibraltar, *Deep Sea Res., Part I or Part II*, **16**, 479–487.
- Ziegenein, J. (1970), Spatial observations of short internal waves in the Strait of Gibraltar, *Deep Sea Res., Part I or Part II*, **17**, 867–875.
- 
- A. Baquerizo, Grupo de Puertos y Costas, University of Granada, Granada, Spain. (abaqueri@ugr.es)
- F. Criado Aldeanueva, J. García Lafuente, and J. C. Sánchez Garrido, Grupo de Oceanografía Física, Department of Applied Physics II, ETSI Telecomunicación, University of Málaga, Campus de Teatinos s/n, Málaga 29071, Spain. (jcsanchez@ctima.uma.es)
- G. Sannino, Climate Department, ENEA, C.R. Casaccia, Rome, Italy. (gianmaria.sannino@casaccia.enea.it)